



Title	An intraplate slow earthquake observed by a dense GPS network in Hokkaido, northernmost Japan
Author(s)	Ohzono, Mako; Takahashi, Hiroaki; Ichiyonagi, Masayoshi
Citation	Geophysical Journal International, 200(1), 144-148 https://doi.org/10.1093/gji/ggu380
Issue Date	2015-01
Doc URL	http://hdl.handle.net/2115/58571
Rights	This article has been accepted for publication in "Geophysical Journal International" © The Authors 2015. Published by Oxford University Press on behalf of The Royal Astronomical Society.
Type	article
File Information	GJI_200_p144-.pdf



[Instructions for use](#)

EXPRESS LETTER

An intraplate slow earthquake observed by a dense GPS network in Hokkaido, northernmost Japan

Mako Ohzono,¹ Hiroaki Takahashi² and Masayoshi Ichiyanagi²

¹*Department of Earth and Environmental Sciences, Faculty of Science, Yamagata University, 1-4-12 Kojirakawa-machi, Yamagata 990-8560, Japan. E-mail: m-ohzono@sci.kj.yamagata-u.ac.jp*

²*Institute of Seismology and Volcanology, Graduate School of Science, Hokkaido University, Kita 10 Nishi 8, Kita-ku, Sapporo 060-0810, Japan*

Accepted 2014 September 26. Received 2014 September 23; in original form 2014 April 24

SUMMARY

An intraplate slow earthquake was detected in northernmost Hokkaido, Japan, by a dense network of the global navigation satellite system. Transient abnormal acceleration of <12 mm was observed during the period 2012 July to 2013 January (~5.5 months) at several sites. The spatial displacement distribution suggests that a localized tectonic event caused localized deformation. Estimated fault parameter indicates very shallow-dip reverse faulting in the uppermost crust, with a total seismic moment of $1.75E + 17$ N m (M_w 5.4). This fault geometry is probably consistent with detachment structure indicated by geological studies. A simultaneous earthquake swarm with the maximum magnitude $M4.1$ suggests a possibility that the slow slip triggered the seismic activity for unknown reasons. This slow earthquake is slower than its moment would indicate, with a duration–magnitude scaling relationship unlike either regular earthquakes or subduction slow slip events. This result indicates that even if the area is under different physical property from subduction zones, slow earthquake can occur by some causes. Slow earthquakes exist in remote regions away from subduction zones and might play an important role in strain release and tectonic activity.

Key words: Satellite geodesy; Transient deformation; Creep and deformation; Intraplate processes; Dynamics and mechanics of faulting; High strain deformation zones.

1 INTRODUCTION

Discoveries of slow slip events (SSEs) in various geodetic and seismological data have been reported in several subduction zones [e.g. Rogers & Dragert (2003) in Cascadia, Canada; Obara *et al.* (2004) in the Nankai Trough, Japan; Wallace & Beavan (2006) in Hikurangi, New Zealand; Ohta *et al.* (2006) in Alaska, United States] and at non-subduction plate boundaries [e.g. Linde *et al.* (1996) on the San Andreas Fault; Murase *et al.* (2013) on the Longitudinal Valley Fault, Taiwan]. A diagram presented by Ide *et al.* (2007) shows seismic moment versus slip duration during an SSE. They clearly indicate a scaling relationship of slow earthquakes is differs from that of ordinary earthquakes. Accordingly, Ide *et al.* (2007) argued that unified physical mechanics governing SSEs generate an independent scaling law.

Global SSE distributions demonstrate that few such events occur outside plate boundaries (Ide *et al.* 2007; Gao *et al.* 2012). This suggests these slow events could be uniquely associated with mature tectonic boundaries such as subduction zones. However, it is possible that we have missed small seismic signals and weak geodetic signals associated with local SSEs outside of subduction zones. It is

worth noting that capturing all SSE data in a region is rare without sufficient observation tools and conditions. This fact implies that SSE distribution may be more widespread than we know, and suggests that the unique association of slow events with surrounding tectonics may be an erroneous perception. Therefore, dense, highly sensitive, continuous geodetic networks should be checked for SSE detection.

Northern Hokkaido in Japan is located in the broad boundary zone between the continental Amur and Okhotsk micro plates (e.g. Seno *et al.* 1996; Heki *et al.* 1999). Over a century of geodetic observations have detected steady east–west compression of about 2×10^{-7} strain yr^{-1} (Ishikawa & Hashimoto 1999). Fig. 1 shows the horizontal velocity and strain rate field observed from 2007 to 2009 by the nationwide global navigation satellite system (GNSS), which is operated by the Geospatial Information Authority of Japan (GSI). Recent global positioning system (GPS) data in northern Hokkaido (Fig. 1) and in the nearby region of Sakhalin (Vasilenko & Prytkov 2012) indicate a similar strain rate. Focal mechanisms of local earthquakes have also indicated east–west compressional reverse faulting (Takahashi & Kasahara 2005). These regional data might reflect the convergence of plates. Several

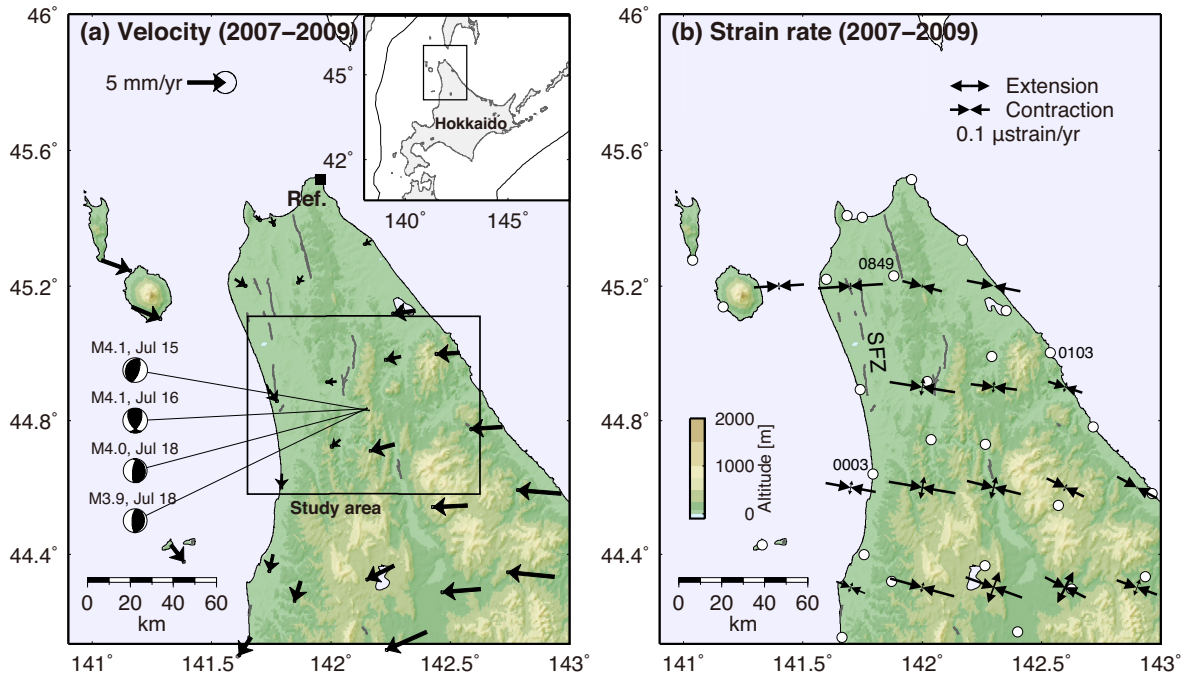


Figure 1. (a) Interseismic (period: 2007 June 11–2011 March 10) horizontal velocity with respect to site 0848 (Wakkanai3, shown as Ref.), estimated from daily coordinates of GSI network. Error ellipsoids indicate 1σ . Focal mechanisms are provided by the National Research Institute for Earth Science and Disaster Prevention (F-net). Grey solid lines are traces of the Quaternary active faults. (b) Principal strain rate axis distribution calculated from horizontal velocities shown in (a), using the method of Sagiya *et al.* (2000) (distance decay constant = 20 km). Open circles are locations of GSI sites. Daily coordinates of three numbering sites are constrained when the coordinate estimation. SFZ indicates the Sarobetsu fault zone.

active faults strike north–south in northern Hokkaido, but estimation of plate boundaries is difficult because no historical records of large earthquakes exist. However, 30-yr large earthquake occurrence probability on the Sarobetsu active fault zone (SFZ in Fig. 1b) is estimated ≤ 4 per cent. This value is higher than most inland active faults in Japan (Headquarters for Earthquake Research Promotion, <http://www.jishin.go.jp/main/index-e.html>). The diffuse distribution of active structures could suggest broad convergence over a 100 km.

Since 2007, Hokkaido University has operated a dense GPS array in the northernmost Hokkaido to monitor crustal deformation. GSI also operates GNSS network in this area, distributed at ~ 25 km intervals (white circles in Fig. 1b). The combined Hokkaido University and GSI networks have a site spacing of about 10 km. In this dense network, several GPS sites began recording anomalous gradual signals in coordinate time-series in 2012 July, which continued for ~ 5.5 months. During this geodetic event, slight seismic activity was also observed. Earthquake swarm with maximum magnitude $M4.1$ began on 2012 July 15, and lasted for a few months at shallow (~ 5 km depth) southeast part of those GPS sites (Ichiyanagi *et al.* 2012). In this study, we analysed GPS data to extract SSE signals and propose a fault model that explains crustal deformation.

2 GPS DATA AND FAULT ESTIMATION

GPS data were analysed using Bernese GPS Software version 5.0 (Dach *et al.* 2007) with International GNSS Service (IGS) precise orbit and Earth orientation parameters. Daily coordinates at each site were estimated by the double-difference method, with the hard constraint of daily coordinates from three GSI sites (0003, 0103

and 0849, Fig. 1b). Those coordinates were provided by GSI as F3 coordinates (<http://terras.gsi.go.jp>).

Fig. 2 shows the daily baseline length change with respect to site 0103 from 2007 June to 2014 June (2007.4–2014.4) at seven GPS sites. To see more long-term time-series, after the SSE, the baseline length change calculated from F3 coordinates are also plotted for two GEONET sites (0851 and 0104, light red in Fig. 2). The coordinate fluctuation during the winter season that is apparent from GPS sites HIAN, MCNS and SRKM resulted from snow cover on antennas. Therefore, in the following discussions, we did not use data collected in winter. Because of problematic site environments, signals from sites DNNP in 2011 were judged artificial. Although significant annual and semi-annual trends contaminate the time-series in DNNP and NUBS, steep contraction can be detected as same as 0851 from middle of 2012 to beginning of 2013 (shaded period in Fig. 2).

To extract regional deformation, coordinates were converted to local movement with respect to site 0103. For the displacement signal extraction, linear, annual, and semi-annual trends were estimated during the period from 2007 to 2011 March 10 (the day before the 2011 $M9.0$ Tohoku Earthquake) and eliminated from the time-series. The coseismic step of the 2011 Tohoku Earthquake and artificial steps caused by maintenance were also eliminated.

The horizontal displacement field during this event is shown in Fig. 3(a) with black vectors. These displacements were calculated from differences in 3-d, averaged coordinates before 2012 July 15 and after 2013 January 3. It is clear that there is a transient abnormal displacement around this period. However, detection of the strict beginning and end times of this event is difficult. In this study, we tentatively chose the beginning of the earthquake swarm as the beginning of transient displacement, and the final date was at the occurrence of an $M4.7$ earthquake in the

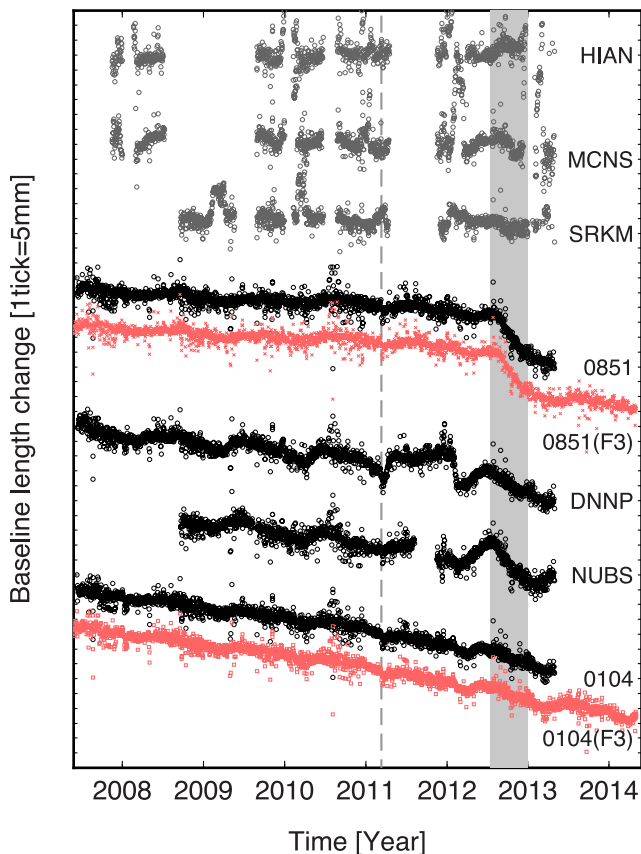


Figure 2. Daily baseline length change compared to site 0103 (Esashi) from 2007 June to 2014 June (2007.4–2014.4). For GEONET sites 0851 and 0104, baseline length change calculated from F3 coordinates are also plotted in light red. Site locations are shown in Fig. 3(a). The dashed line is the timing of the 2011 Tohoku earthquake. The shadowed period (2012.5369–2013.0068) corresponds to the SSE duration.

western part of the GPS network (National Research Institute for Earth Science and Disaster Prevention, <http://www.fnet.bosai.go.jp/fnet/event/tdmt.php?ID=20130103111300&LANG=en>). Epicentre distributions are plotted on Fig. 3(a) from 2012 July 15 to 2013 January 31. Hypocentre distributions are also shown in Figs 3(b) and (c) with occurrence time. Coincidentally, duration of the transient displacement almost agree with this period.

A coherent, gradual, eastward and abnormal displacement appears at sites 0851, DNNP and NUBS. No clear signals were observed at other sites and during other periods. Site 0851 recorded the largest displacement, with 11.7 ± 2.6 mm of eastward movement and 3.4 ± 3.6 mm of southward movement. The displacement direction is consistent with the well-resolved strain and stress field developed by geodetic and focal mechanisms of local earthquakes. Two reasons suggest these signals are due to local SSE phenomena: (1) the area of coherent displacement (20–30 km in width) is too broad to suspect shallow hydrologic phenomena and (2) there are several geological boundaries, including an active fault (e.g. Toikanbetsu fault, Fig. 3a), under the east–west compressional tectonic field. We therefore assert that this signal was a tectonic SSE. The deformation shown in Fig. 3(a) indicates local displacement distribution. In addition, it suggests shallow fault activity, which affects only limited areas.

To explain this crustal deformation, we estimated fault parameters using a nonlinear inversion method (Matsu'ura & Hasegawa

1987). Using information about the geological structure (e.g. Yamamoto 1979) and geometry of active faults in this region (National Institute of Advanced Industrial Science and Technology, https://gbank.gsj.jp/activefault/index_e_gmap.html), we constrained the fault geometry to a north–south strike and west dip as an *a priori* parameter. There are three candidates of the SSE fault: the Toikanbetsu fault, detachment fault along geological structure, and trace of hypocentres distribution during this period. We tried all fault geometries as *a priori* parameters and inverted them through a trial and error process to minimize the residuals. As a result, the estimated fault became a very shallow, west-dipping reverse fault in the uppermost crust (Fig. 3). The estimated parameters are listed in Table 1. The released moment was expected to be $1.75E + 17$ N m (M_w 5.4) for a rigidity of 30 GPa. The estimated fault appears to connect to the active Toikanbetsu fault (TF in Fig. 3). This suggests a possibility of a relationship between the observed SSE and the Toikanbetsu fault. Additionally, estimated fault is located just above the earthquake swarm in 2012 July (Figs 3b and c). It is also considerable matter of the relationship between them.

3 DISCUSSION

The estimated fault geometry of the east–west compressional reverse fault agrees well with the secular strain field (Fig. 1) and the focal mechanisms of local earthquakes (e.g. Takahashi & Kasahara 2005). This suggests that the release style of the SSE was one of accumulated strain due to the diverse convergence of the Amur and Okhotsk plates (e.g. Heki *et al.* 1999).

A weak earthquake swarm, with magnitudes no larger than $M4.1$, coincided with the beginning of the SSE. Hypocentres derived from temporal seismic observations (Ichiyanagi *et al.* 2012) were located in and around the estimated fault during the period from 2012 July to 2012 September (Fig. 3). The rather large seismic moment of the SSE, compared to the seismic activity, possibly indicates that the SSE governed and triggered the seismic activity.

In a geological investigation of the area, Yamamoto (1979) suggested an active anticline structure caused by a detachment fault. Our estimated SSE fault geometry (very shallow dip angle in the uppermost part of the crust) is in good agreement with this detachment structure. The existence of the active Toikanbetsu fault connects to the estimated fault may also suggest a strong connection between the SSE and the active geological structure.

Yoshida & Kato (2003) modelled the occurrence of slow slip when stress reaches a steady state level with a stability transition of frictional parameters, using a two-degrees-of-freedom, block-spring model. Their model also required a stress build-up within the background region, including the main fault system. Instrumental and historical records indicate that this region has been a seismic gap for more than 300 yr. Thus, the SSE may conceivably be an indicator of stress build-up, raising the possibility of a large earthquake in the near future.

Estimated static fault parameters (length, width and dislocation) are in good agreement with the scaling law from inland earthquakes of the Japanese Islands (e.g. Matsuda 1975). However, the relationship between duration and seismic moment differs from the unified scaling law of slow events summarized by Ide *et al.* (2007) and Gao *et al.* (2012) (Fig. 4). A few SSEs at shallow non-subduction zone are detected at the San Andreas Fault (SAF; e.g. Linde *et al.* 1996) and Hawaii (Segall *et al.* 2006). The SSE at SAF also does not on the scaling law. There is an idea that this discrepancy is a result of natural variation caused by estimation

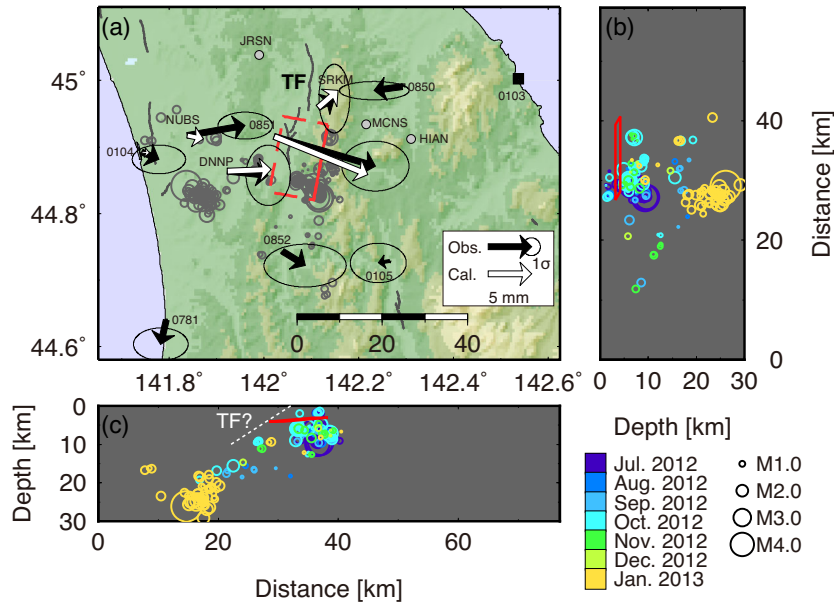


Figure 3. (a) Observed (black) and calculated (white) horizontal displacements during the SSE (2012 July 15–2013 January 3). Error ellipsoids of the observations indicate 1σ . Grey open circles are epicentres of the earthquake swarm observed by temporal dense seismic network since 2012 July 15 until 2013 January 31 (Ichiyanagi *et al.* 2012). A red rectangle denotes the surface trace of the estimated fault. The solid line indicates the upper edge. Grey solid lines are traces of the Quaternary active faults. TF shows the Toikanbetsu active fault. Grey circles denote locations of GPS sites JRSN, MCNS and HIAN, which were not used in this study. (b) and (c) Cross-section of the hypocentre distribution. Colour indicates the timing of the earthquakes. The solid red line corresponds to the location of the estimated SSE fault.

Table 1. Estimated fault parameters.

Longitude ^a (°)	Latitude ^a (°)	Depth ^a (km)	Length (km)	Width (km)	Strike (°)	Dip (°)	Rake (°)	Slip (m)
142.1345	44.9340	3.1	12.8	7.6	190.4	7.8	87.0	0.06

^aLocation indicates upper north edge of the fault.

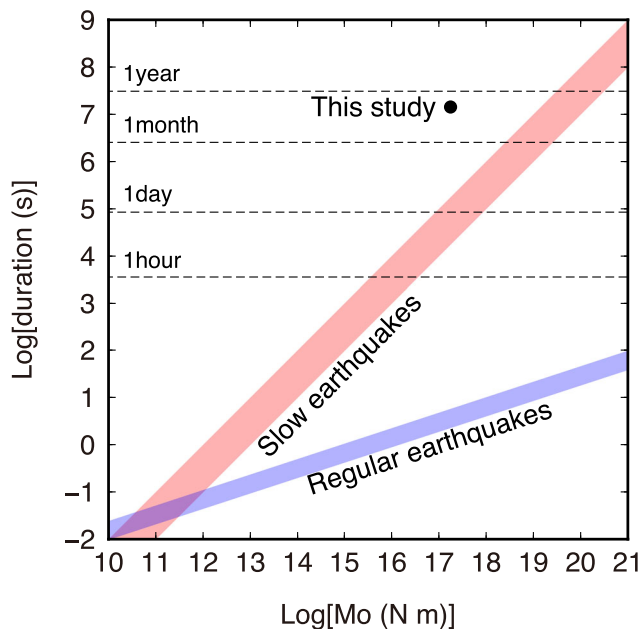


Figure 4. Relationship between the seismic moment and event duration on a logarithmic scale. The solid circle represents the study results. Ranges of the slow earthquakes (red) and regular earthquakes (blue) are based on Ide *et al.* (2007) and Gao *et al.* (2012).

errors (e.g. Peng & Gomberg 2010). However, our estimation clearly away from the scaling law, therefore it could possibly reflect an unrecorded SSE series in non-subduction zones. Gao *et al.* (2012) also compiled a relationship among the SSE's seismic moment, fault area and static stress drop. They show that static stress drop for shallow SSEs are higher than those of subduction zones. The static stress drop of our estimated SSE also has similar value with the SAF and Hawaiian cases (0.1–1 MPa). As Gao *et al.* (2012) pointed out, low pore fluid pressure at shallow SSE region probably requires larger stress drop than that of subduction zones, which have small shear stress under high pore fluid pressure. Shallow source depth also gives different physical property (e.g. temperature and pressure) compared with deep SSE in subduction zones. This divergence from ordinary SSE scaling might suggest that a variety of sedimentary materials could control the frictional constructive law of inland SSEs.

4 CONCLUSIONS

A dense GPS array near a plate boundary detected an SSE during a ~ 5.5 months period beginning in 2012 July in Hokkaido, Japan, where diffuse convergence of the Amur and Okhotsk continental plates has been observed. These slow events appear to occur not only at mature plate boundaries, but also in regions where tectonic stress is actively increasing. An estimated static fault with $M_w 5.4$

conforms well to crustal deformation data. The seismic moment of the SSE was somewhat larger than the seismic moment of simultaneous seismic activity. The estimated fault geometry agreed with a possible detachment fault inferred from a geological investigation in the area. Static fault parameters were consistent with known scaling of inland earthquakes. Dynamic parameters for the SSE duration and released seismic moment, however, differ from the scaling law of slow earthquakes. SSEs are possibly an indicator of stress build-up that can be released in an earthquake. The stress build-up is inferred from experimental simulations, which agree well with the existence of a seismic gap during more than 300 yr of steady-strain accumulation ($1\text{--}2 \times 10^{-7}$ strain yr^{-1}). These results suggest that stress build-up processes may occur before large earthquakes in this region.

ACKNOWLEDGEMENTS

We thank GSI for GEONET data and the National Research Institute for Earth Science and Disaster Prevention for F-net data. The manuscript is improved by efforts and useful comments of Editor Dr Jeannot Trampert and two reviewers, Dr Abhijit Ghosh and an anonymous reviewer. We used Generic Mapping Tools (Wessel *et al.* 2013) to create the figures herein. This research is supported by JSPS KAKENHI 25257204, JSPS Bilateral Program and the Ministry of Education, Culture, Sports, Science and Technology (MEXT) of Japan, under its Earthquake and Volcano Hazards Observation and Research Program.

REFERENCES

- Dach, R., Hugentobler, U., Fridez, P. & Meindl, M., 2007. *Bernese GPS Software version 5.0*, Astronomical Institute, University of Bern, pp. 612.
- Gao, H., Schmidt, D.A. & Weldon, R.J. II, 2012. Scaling relationships of source parameters for slow slip events, *Bull. seism. Soc. Am.*, **102**(1), 352–360.
- Heki, K. *et al.*, 1999. The Amurian plate motion and current plate kinematics in eastern Asia, *J. geophys. Res.*, **104**, 29 147–29 155.
- Ichiyanagi, M. *et al.*, 2012. Inland seismic activity of Hokkaido after the 2011 Tohoku earthquake (M9.0), in *Proceedings of the Fall Meeting of the Seismological Society of Japan*, Hakodate, Hokkaido Japan, Abstract P3-05 (in Japanese).
- Ide, S., Beroza, G.C., Shelly, D. & Uchide, T., 2007. A scaling law for slow earthquakes, *Nature*, **447**, 76–79.
- Ishikawa, N. & Hashimoto, M., 1999. Average horizontal crustal strain rates in Japan during interseismic period deduced from geodetic surveys (Part 2), *Zisin*, **52**, 299–315 (in Japanese with English abstract).
- Linde, A.T., Gladwin, M.T., Johnston, M.J.S., Gwyther, R.L. & Bilham, R.G., 1996. A slow earthquake sequence on the San Andreas Fault, *Nature*, **383**, 65–68.
- Matsuda, T., 1975. Magnitude and recurrence interval of earthquakes from a fault, *Zisin*, **28**, 269–283 (in Japanese with English abstract).
- Matsu'ura, M. & Hasegawa, Y., 1987. A maximum likelihood approach to nonlinear inversion under constraints, *Phys. Earth planet. Int.*, **47**, 179–187.
- Murase, M., Matta, N., Lin, C-H., Chen, W-S. & Koizumi, N., 2013. An episodic creep-slip event detected by precise levelling surveys in the central part of the Longitudinal Valley Fault, eastern Taiwan, in 2011–2012, *Tectonophysics*, **608**, 904–913.
- Obara, K., Hirose, H., Yamamizu, F. & Kasahara, K., 2004. Episodic slow slip events accompanied by non-volcanic tremors in south-west Japan subduction zone, *Geophys. Res. Lett.*, **31**(23), L23602, doi:10.1029/2004GL020848.
- Ohta, Y., Freymueller, J.T., Hreinsdóttir, S. & Suito, H., 2006. A large slow slip event and the depth of the seismogenic zone in the south central Alaska subduction zone, *Earth planet. Sci. Lett.*, **247**(1–2), 108–116.
- Peng, Z. & Gombert, J., 2010. An intergrated perspective of the continuum between earthquakes and slow-slip phenomena, *Nat. Geosci.*, **3**, 599–607.
- Rogers, G. & Dragert, H., 2003. Episodic tremor and slip on the Cascadia subduction zone: The chatter of silent slip, *Science*, **300**, 1942–1943.
- Sagiya, T., Miyazaki, S. & Tada, T., 2000. Continuous GPS array and present-day crustal deformation of Japan, *Pure appl. Geophys.*, **157**, 2303–2322.
- Segall, P., Desmarais, M.K., Shelly, D., Miklius, A. & Cervelli, P., 2006. Earthquakes triggered by silent slip events on Kilauea volcano, Hawaii, *Nature*, **44**, 71–74.
- Seno, T., Sakurai, T. & Stein, S., 1996. Can the Okhotsk plate be discriminated from the North American plate?, *J. geophys. Res.*, **101**(B5), 11 305–11 315.
- Takahashi, H. & Kasahara, M., 2005. Seismic activity in the coastal area of Rumoi subprefecture and tectonics in Northern Hokkaido, Japan, *Geophys. Bull. Hokkaido Univ.*, **68**, 199–218 (in Japanese with English abstract).
- Vasilenko, N.F. & Prytkov, A.S., 2012. GPS-based modeling of the interaction between the lithospheric plates in Sakhalin, *Russ. J. Pacific Geol.*, **6**(1), 35–41.
- Wallace, L.M. & Beavan, J. 2006. A large slow slip event on the central Hikurangi subduction interface beneath the Manawatu region, North Island, New Zealand, *Geophys. Res. Lett.*, **33**(11), L11301, doi:10.1029/2006GL026009.
- Wessel, P., Smith, W.H.F., Scharroo, R., Luis, J.F. & Wobbe, F., 2013. Generic mapping tools: improved version released, *EOS, Trans. Am. geophys. Un.*, **94**, 409–410.
- Yamamoto, H., 1979. The geologic structure and the sedimentary basins off northern part of the Hokkaido island, *J. Jap. Assoc. Petro. Tech.*, **44**(5), 28–35 (in Japanese with English abstract).
- Yoshida, S. & Kato, N., 2003. Episodic aseismic slip in a two-degree-of-freedom block spring model, *Geophys. Res. Lett.*, **30**, 1681, doi:1029/2003GL017439.